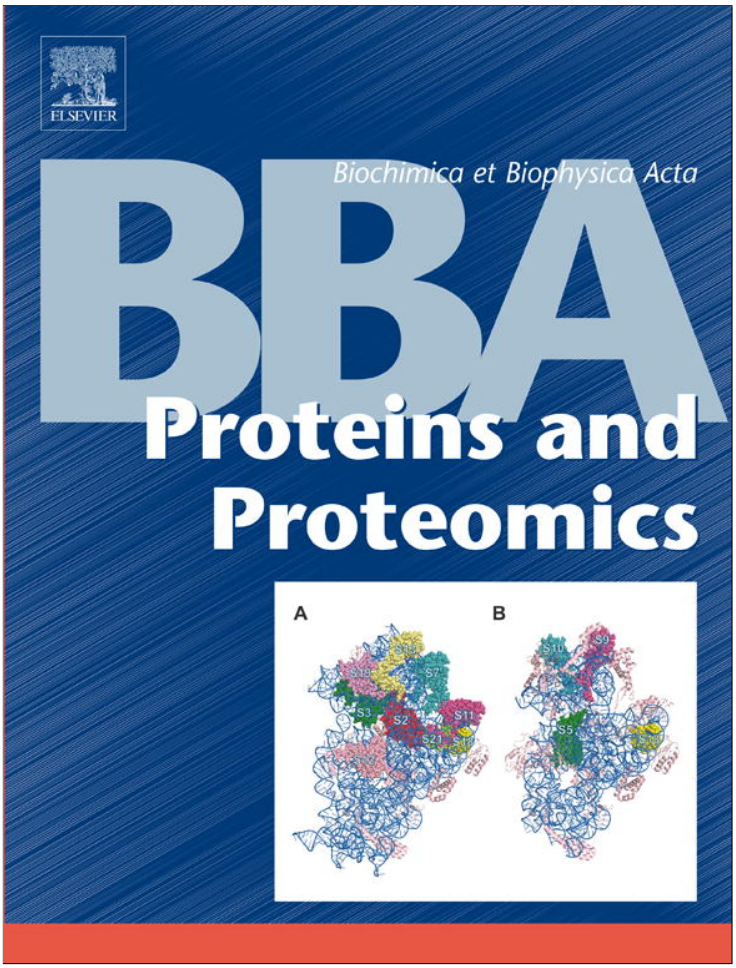

(This is a sample cover image for this issue. The actual cover is not yet available at this time.)

Biochimica et Biophysica Acta 1834 (2013) 629–633

Contents lists available at SciVerse ScienceDirect

Biochimica et Biophysica Acta

journal homepage: www.elsevier.com/locate/bbapap

Influencing the monophenolase/diphenolase activity ratio in tyrosinase

Mor Goldfeder [a], Margarita Kanteev [a], Noam Adir [b], Ayelet Fishman [a,*]

[a] Department of Biotechnology and Food Engineering, Technion-Israel Institute of Technology, Haifa 32000, Israel
[b] Schulich Faculty of Chemistry, Technion-Israel Institute of Technology, Haifa 32000, Israel

ARTICLE INFO

Article history:
Received 10 November 2012
Received in revised form 27 December 2012
Accepted 28 December 2012
Available online 8 January 2013

Keywords:
Tyrosinase
Bacillus megaterium
Rational design
Diphenol
Copper

ABSTRACT

Tyrosinase is a type 3 copper enzyme with great potential for production of commercially valuable diphenols from monophenols. However, the use of tyrosinase is limited by its further oxidation of diphenols to quinones. We recently determined the structure of the *Bacillus megaterium* tyrosinase revealing a residue, V218, which we proposed to take part in positioning of substrates within the active site. In the structure of catechol oxidase from *Ipomoea batatas*, the lack of monophenolase activity was attributed to the presence of F261 near CuA. Consequently, we engineered two variants, V218F and V218G. V218F was expected to have a decreased monophenolase activity, due to the bulky residue extending into the active site. Surprisingly, both V218F and V218G exhibited a 9- and 4.4-fold higher monophenolase/diphenolase activity ratio, respectively. X-ray structures of variant V218F display a flexibility of the phenylalanine residue along with an adjacent histidine, which we propose to be the source of the change in activity ratio.

1. Introduction

Tyrosinases (EC 1.14.18.1) are type 3 copper proteins able to perform two successive reactions in the presence of molecular oxygen; the hydroxylation of phenols to form *ortho*-diphenols (monophenolase activity), and the oxidation of *o*-diphenols to *o*-quinones (diphenolase activity) [1,2]. The resulting highly reactive *ortho*-quinones autopolymerize to melanin, accountable for skin pigmentation and fruit and vegetable browning. Tyrosinases have a highly conserved active site albeit their wide distribution throughout evolution [3–7]. The active site comprises six histidine residues which coordinate the two copper ions CuA and CuB [1,8]. Along with tyrosinases, the type 3 copper protein family includes catechol oxidase which performs only the oxidation of diphenols, and hemocyanins, which are oxygen carriers from the hemolymph of many molluscs and arthropods [9–11].

The ability of tyrosinases to convert monophenols into diphenols has stimulated studies regarding the production of various *ortho*-diphenols (also referred to as substituted catechols). Catechols are important intermediates for the synthesis of pharmaceuticals, agrochemicals, flavors, polymerization inhibitors, and antioxidants [12–16]. Despite the great potential, the use of tyrosinases for catechol synthesis has been limited since their diphenolase activity is much higher than their monophenolase activity [17]. In nature, there is a single reported unique bacterial tyrosinase from *Ralstonia solanacearum* with an abnormally high tyrosine hydroxylation/L-Dopa oxidation ratio [17]. Recently, we employed directed evolution on a tyrosinase from the soil bacterium *Bacillus megaterium* (TyrBm) in an attempt to alter the selectivity of the enzyme [18,19]. Variant R209H exhibited a monophenolase/diphenolase activity ratio 2.6-fold higher than the wild type (WT) enzyme. The crystal structures of both wild-type TyrBm and variant R209H have been recently determined [20], and it was discovered that arginine at position 209 exhibits alternative conformations and is a critical residue located in the entrance to the active site. The structure further revealed a residue, V218, situated on a loop above CuA, which extends into the active site. This paper describes the rational mutagenesis preformed on residue V218, and the significant effect it has on the activity and selectivity of TyrBm.

2. Materials and methods

2.1. Reagents and materials

L-3,4-dihydroxyphenylalanine (L-Dopa) was purchased from Acros (Geel, Belgium). L-tyrosine, kanamycin, imidazole, trizma base, and sodium cacodylate trihydrate were purchased from Sigma-Aldrich Chemical Co. (Sigma-Aldrich, Rehovot, Israel). $CuSO_4$ was purchased from Merck (New Jersey, USA). All materials used were of the highest purity available and were employed without further purification.

2.2. Expression and purification of tyrosinase from B. megaterium

A tyrosinase producing *B. megaterium* (TyrBm) was isolated from soil samples and the gene encoding for the tyrosinase was cloned into *Escherichia coli* BL21. The enzyme was expressed and purified as previously described [19,21]. Variants V218F and V218G were

Abbreviations: L-Dopa, L-3,4-dihydroxyphenylalanine; TyrBm, tyrosinase from *Bacillus megaterium*

* Corresponding author. Tel.: +972 4 829 5898; fax: +972 4 829 3399.
E-mail address: afishman@tx.technion.ac.il (A. Fishman).

1570-9639/$ – see front matter © 2013 Elsevier B.V. All rights reserved.
http://dx.doi.org/10.1016/j.bbapap.2012.12.021

created by QuickChange® site-directed mutagenesis kit (Stratagene, CA, USA) as suggested by the manufacturer using the primers listed in Supplementary Table 1. Verification of the mutations was obtained by sequencing. Purification steps were identical to those performed on the WT.

2.3. Kinetic characterization of variants V218F and V218G on L-tyrosine and L-Dopa

Tyrosinase monophenolase and diphenolase activity was determined by measuring the formation of L-dopachrome from L-tyrosine or L-Dopa. The values of K_m and V_{max} for the purified tyrosinase variants and the wild-type enzyme were determined by a colorimetric assay with the following conditions: 200 μl 50 mM Tris HCl buffer pH 7.5, 0.01 mM $CuSO_4$, 28 °C, employing 3 μg ml^{-1} of purified enzyme, and substrate concentrations ranging from 0.1 to 6.0 mM for L-Dopa, and 0.02–6.0 mM for L-tyrosine. The formation of L-dopachrome ($\varepsilon = 3600\ M^{-1}\ cm^{-1}$) was monitored by measuring the absorbance at 475 nm [22]. All measurements were performed in triplicates in 96-well plates at 25 °C and monitored with a multi-plate reader (OPTImax tunable microplate reader; Molecular Devices, Sunnyvale, CA., USA). The light path was determined as 0.68 cm.

2.4. Crystallization, data collection, and structure determination

TyrBm variants were crystallized as previously described [21]. Mature crystals were soaked in 1 mM $CuSO_4$ for 2 h after which they were mounted on a loop and frozen. X-ray diffraction data was collected at the European Synchrotron Radiation Facility (ESRF), Grenoble, France, beamlines ID 23-1. All data were indexed, integrated, scaled and merged using Mosflm and Scala [23]. The structure of TyrBm was solved by molecular replacement (MR) using Phaser [24] and the coordinates of earlier determined TyrBm structure (PDB code 3NM8). A single solution was obtained for two monomers in the asymmetric unit. Refinement was performed using Phenix [25], coupled with rounds of manual model building, real-space refinement and structure validation performed using COOT [26]. Data collection, phasing, and refinement statistics are presented in Table 1.

Table 1
Data collection and refinement statistics.

Structure name (PDB code)	*TyrBm_V218F* (4HD4)	*TyrBm_V218F_Cu* (4HD6)	*TyrBm_V218G_Cu* (4HD7)
X-ray data collection			
Space group	$P2_1$	$P2_1$	$P2_1$
Unit-cell parameters (Å, °)			
a	48.0	48.2	47.9
b	78.6	78.9	78.7
c	85.9	85.8	85.8
α	90	90	90
β	106.1	106.1	105.9
γ	90	90	90
Resolution range	36.5–1.8	41.2–2.0	41.2–2.1
Observed reflections	178,251	95,352	81,798
Unique reflections	54,388	40,762	34,263
$I/\sigma(I)$[a]	9.3 (5.0)	6.6 (3.4)	6.6 (4.1)
R_{merge}[a,b]	0.1 (0.17)	0.07 (0.29)	0.09 (0.18)
Completeness[a]	96.3 (96.3)	97.5 (96.8)	95.9 (98.3)
Multiplicity[a]	3.3 (3.3)	2.3 (2.3)	2.4 (2.4)
Refinement			
R(%)/R_{free}(%)[c]	20.7/22.9	24.5/27.8	25.5/28.4
Amino acids	579	578	578
Total number of non-hydrogen atoms	4956	4966	4914
Number of water molecules	236	254	214
Number of copper ions	1	2	2
Average *B* factor (Å), protein atoms	16.2	25.9	26.4
r.m.s.d			
Bond length (Å)	0.01	0.012	0.012
Bond angle (°)	1.2	1.2	1.2
Ramachandran plot			
Favored regions (%)	97.5	95.8	96.8
Outliers (%)	0.2	0.0	0.4

[a] Values in parentheses are for the last shell.
[b] $R_{merge} = \sum_{hkl}\sum_i |I_i(hkl) - \langle I(hkl)\rangle| / \sum_{hkl}\sum_i I_i(hkl)$, where I is the observed intensity, and $\langle I \rangle$ is the mean value of I.
[c] $R/R_{free} = \sum_{hkl}||F_{obs}| - |F_{calc}|| / \sum_{hkl}|F_{obs}|$ where R and R_{free} are calculated using the test reflections respectively. The test reflections (5%) were held aside and not used during the entire refinement process.

2.5. Protein Data Bank accession numbers

Coordinates and structure factors of TyrBm have been deposited in the RCSB Protein Data Bank under accession codes 4HD4 for *TyrBm_V218F*, 4HD6 for *TyrBm_V218F_Cu* and 4HD7 for *TyrBm_V218G_Cu*.

3. Results and discussion

3.1. TyrBm variants V218F and V218G and their activity

Analysis of the recently determined crystal structures of WT TyrBm [20] suggested that residue V218 might modulate substrate and product specificity. It is situated on a loop above CuA, which extends into the entrance to the active site, occupying the same location as F261 in catechol oxidase from *Ipomoea batatas* (Sweet potato) [11]. We recently proposed that V218 can be a "gate-keeper" residue, controlling the entrance of ligands to the active site of TyrBm [20]. It was further suggested that since valine is less bulky than phenylalanine, it allows the hydroxylation of monophenols on CuA, which does not occur in catechol oxidase. The homologous loop in tyrosinase from *Streptomyces castaneoglobisporus* (TyrSc), for which a structure in complex with a caddie protein is available, is shorter and located farther from the active site, with the smaller G204 occupying the analogous position of V218 [27]. In the recently determined structure of *Agaricus bisporus* (a mushroom) tyrosinase in complex with the inhibitor tropolone, the homologous position V283 is observed within van der Waals distance from the ligand (about 3.7 Å) [28]. In order to examine the propositions made for residue V218, and to elucidate its role in tyrosinase activity, the valine residue was mutated to either phenylalanine (V218F) or glycine (V218G).

Due to the substitution of the smaller valine side chain with the bulkier phenylalanine, we expected a reduction in the activities of the TyrBm variant V218F, especially the monophenolase activity. Surprisingly, the V218F variant's monophenolase activity on L-tyrosine improved, as the V_{max} and k_{cat} values increased 4.2-fold (from 6.8 to 28.4 μmol min^{-1} mg^{-1} and from 4.0 to 16.7 s^{-1}, respectively). The same values for diphenolase activity on L-Dopa, however, decreased 2.1-fold (from 75.0 to 35.7 μmol min^{-1} mg^{-1} and from 44.1 to 21.0 s^{-1}, respectively). Overall, the monophenolase/diphenolase activity ratio increased by 9-fold (Table 2). This result contradicts a previously suggested proposal that an aromatic residue at this position, such as in sweet potato catechol oxidase, will block CuA and thus eliminate the ability of the enzyme to perform hydroxylation of monophenols [7,29].

In the V218G variant, the increase in the active site volume was expected to improve the activity towards both substrates, and indeed the V_{max} and k_{cat} towards L-tyrosine increased by 7.8-fold and towards L-Dopa by 1.7-fold (Table 2 and Fig. 1). Overall, the monophenolase/diphenolase activity ratio increased by 4.4-fold (0.08 vs. 0.2, respectively). These significant improvements in k_{cat} of both variants were accompanied with a decrease in the affinity of the enzymes towards the substrates, especially towards L-tyrosine. The K_m for tyrosine increased by 28-fold in V218F and by 10-fold in

Table 2
Kinetic constants of WT TyrBm and variants V218F and V218G.

		K_m (mM)	V_{max} (μmol min^{-1} mg^{-1})	k_{cat} (s^{-1})	k_{cat}/K_m (s^{-1} mM^{-1})	V_{max}Mono/ V_{max}Di
WT	L-tyrosine	0.05 ± 0.01	6.8 ± 0.4	4.0	80.0	0.09
	L-Dopa	0.8 ± 0.1	75.0 ± 7.8	44.1	55.1	
V218F	L-tyrosine	1.4 ± 0.1	28.4 ± 0.7	16.7	11.9	0.8
	L-Dopa	1.1 ± 0.3	35.7 ± 7.3	21.0	19.1	
V218G	L-tyrosine	0.5 ± 0.1	52.8 ± 3.2	31.1	62.1	0.4
	L-Dopa	1.0 ± 0.1	124.6 ± 6.7	73.3	73.7	

V218G. A similar phenomena was reported previously for variant R209H, with a 2.6-fold higher mono/diphenolase activity ratio obtained using directed evolution [18].

In mammalian tyrosinase, the analogous residue is also a valine (V377) and on the same loop there is a methionine (M374). It was previously suggested that the peptide oxygen atoms of these two residues serve as hydrogen bond acceptors for the NH-groups of the imidazole ring of two of the copper binding histidines. This loop was therefore suggested as essential for the active site architecture [30]. Olivares et al. mutated residue Q378 of mouse tyrosinase, which is analogous to P219 in TyrBm, on the same loop and adjacent to V218 [6]. Variant Q378H obtained through site-directed mutagenesis had a monophenolase/diphenolase activity ratio 1.9-fold greater than WT, although its affinity (expressed by the value of K_m) towards L-Dopa decreased by 50-fold. The authors suggested that this decrease in affinity is due to the steric hindrance by the imidazole group of H378 which impairs the docking of L-Dopa. Similar steric hindrance may have caused the decreased affinity towards tyrosine in TyrBm variant V218F, although its activity increased.

3.2. Crystal structures of TyrBm variants V218F and V218G

In order to further elucidate the effect of the mutations, the crystal structures of variants V218F and V218G were determined and compared to WT (Fig. 2). High quality data sets were obtained for crystals of both variants. Structures *TyrBm_V218F*, *TyrBm_V218F_Cu* and *TyrBm_V218G_Cu* were determined to a resolution of 1.8 Å, 2.0 Å and 2.1 Å, respectively (the latter two were obtained from crystals soaked in a $CuSO_4$ solution, see Material and methods section for additional details). The overall structures of *TyrBm_V218F*, *TyrBm_V218F_Cu* and *TyrBm_V218G_Cu* are very similar to that of the previously reported WT structure (RMS = 0.3 Å^2) [20].

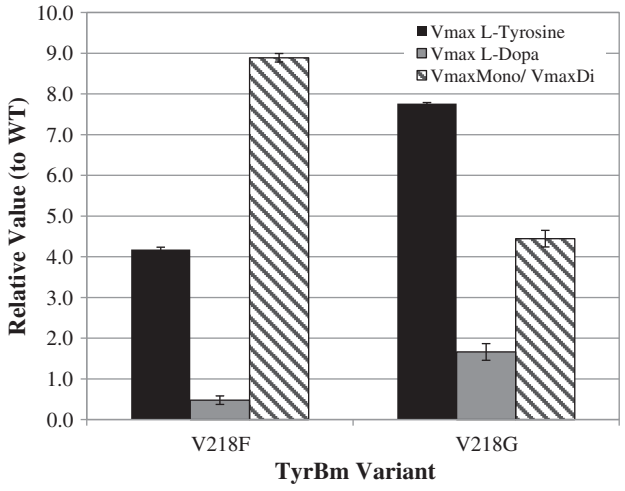

Fig. 1. Relative activity and mono/di-phenolase activity ratio of TyrBm variants. The V_{max} of variants V218F and V218G towards L-tyrosine is significantly higher than that of the WT, while towards L-Dopa there is a decrease in V_{max} of V218F and an increase in V_{max} of V218G. Overall, both variants have increased monophenolase/diphenolase activity ratio. Activity measurements towards L-tyrosine and L-Dopa were determined by monitoring the formation of L-dopachrome at 475 nm.

The biochemical results of this study show that expansion of the active site entrance through position 218, improves the activity on both monophenolic and diphenolic substrates. However, phenylalanine in that position facilitates an increased selectivity towards the monophenol. The determined structures of these variants enable further understanding of these results.

In structure *TyrBm_V218F*, in both subunits, residue F218 is observed in a conformation which is flipped out of the active site (Fig. 2B). This conformation is different than that of F261 in catechol oxidase, which is directed towards the active site. Some electron density was observed in the position above the active site, and could possibly result from an alternate position of F218 (transparent residue in Fig. 2B). However, the electron density was too weak to definitively assign the alternate side chain position. Another residue that is observed in an unexpected conformation is H60, one of the coordinators of CuA. It is also flipped out of the active site (Fig. 2B) while the more common conformation, towards the copper ion, is found only in subunit A at a lower occupancy (about 25%). In a great number of wild type structures of TyrBm obtained by us in the past 2 years, with or without copper ions, this residue was never seen in more than one conformation, but it is known to be flexible as previously shown in the structure of TyrSc [27]. In structure 1WXC of TyrSc, the homologous residue H58, is observed in two alternate conformations, and the authors associated its flexibility to the deprotonation of the substrate tyrosine [27]. The authors further related this histidine's flexibility to the absence of a thioether bond between a cysteine and the histidine, present mostly in catechol oxidases and hemocyanins but also in some tyrosinases. This bond has been suggested to form structural restraints in order to stabilize the copper ions, but since it is absent from most bacterial and mammalian tyrosinases, its role is yet unclear [16,28]. In TyrBm, H60 is one of the closest residues to F218. We therefore suggest that the presence of phenylalanine at position 218 reveals the inherent flexibility of H60 by stabilizing the flipped out conformation in the crystal structure. We can thus concur with the proposal that the flexibility of H60 is indeed essential for TyrBm activity, and that this movement is modified in the V218F variant, thus explaining the change in activity ratio.

The increase in activity of V218F towards tyrosine alongside the decrease towards L-Dopa, can also be related to the common theory that each substrate coordinates to a different copper ion as it enters the active site, tyrosine to CuA and L-Dopa to CuB [8,29]. Ramsden and Riley have recently proposed a mechanism in which the specific coordination of each substrate may have an essential effect on activity [31]. They suggested that diphenols may bind "incorrectly" in the way monophenols bind, and thus lead to an inactivated form of tyrosinase, causing suicide inhibition. Based on this theory, it is possible that the presence of F218 encourages a specific form of tyrosine binding, which leads to improvement in monophenolase activity, while it facilitates incorrect binding of L-Dopa more often, causing the observed decrease in activity. Another possible mechanism of suicide inactivation is proposed by Muñoz-Muñoz et al. [30,32]. They suggest that the transfer of a proton from the hydroxyl at position 2 on the

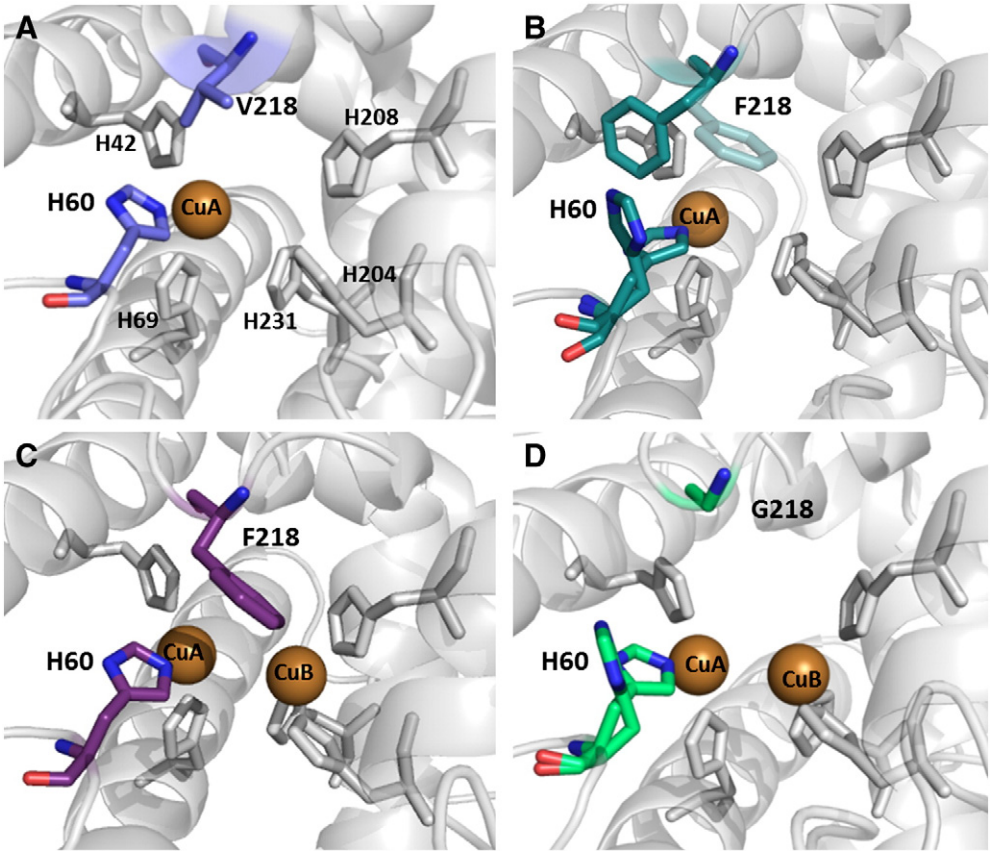

Fig. 2. Structures of TyrBm WT and variants. (A) The active site of WT TyrBm (PDB code 3NM8). Residues V218 and H60 are in stick representation colored in light blue, and nitrogen atoms in dark blue. CuA is shown as a brown sphere while CuB was not present in the structure. (B) The active site of *TyrBm_V218F*. Residues F218 and H60 are in stick representation colored in teal, and nitrogen atoms in dark blue. The alternate conformations of residue H60 are shown. The unassigned electron density conformation of F218 is shown in transparent stick representation. CuA is shown as a brown sphere, while CuB was not present in the structure. (C) The active site of *TyrBm_V218F_Cu*. Residues F218 and H60 are in stick representation colored in purple, and nitrogen atoms in dark blue. CuA and CuB are shown as brown spheres. (D) The active site of *TyrBm_V218G_Cu*. Residues G218 and H60 are in stick representation colored in green, and nitrogen atoms in dark blue. The alternate conformations of residue H60 are shown. CuA and CuB are shown as brown spheres.

phenyl ring of the substrate to the peroxide instead of to a close-by base, causes one copper ion to reduce to Cu(0) and the enzyme to inactivate. It is not unreasonable to assume that F218 may cause slight steric changes within the active site which facilitate the protonation of the peroxide, thus increasing inactivation of the enzyme and decreasing the diphenolase activity observed for this variant. Our experimental results cannot distinguish between the two suicide inactivation mechanisms at this point.

As previously shown in many of the crystal structures of TyrBm, copper ions are often not retained and structures were observed with either one (CuA) (Fig. 2A) or no copper ions [20]. Similarly, in *TyrBm_V218F*, CuB is not observed (Fig. 2B). In *TyrBm_V218F_Cu*, however, the crystals were presoaked in a solution containing 1 mM Cu^{2+} ions, and both CuA and CuB can be identified at 100% occupancy. As can be seen in Fig. 2C, the soak promoted the alternate conformation of F218 which is above the active site, as opposed to that of structure *TyrBm_V218F*. This confirms that F218 is indeed flexible and can be found in two alternate conformations. Furthermore, H60 is observed in this structure only in its most stable conformation, towards CuA. Apparently, the flexibility of these residues is affected by the presence of copper or vice versa, and subsequently it affects the monophenolase activity differently than the diphenolase activity. Since TyrBm does not retain its copper ions, it seems that the copper ion flux into the active site is directly involved in both TyrBm activities.

In the structure of V218G soaked in a copper solution, *TyrBm_V218G_Cu*, the active site volume is significantly increased (Fig. 2D). As a result of the copper soak, both copper ions are present. In one of the subunits, two alternate conformations of H60 are seen, the more stable one at about 66% occupancy and the flipped out conformation at 34%. The increased activity towards L-Dopa can be associated with the enlargement of the active site, spatially enabling faster substrate/product movement. Since the activity on tyrosine was improved significantly by this variant as well, this structure further supports the assumption that the presence of H60 in the flipped out conformation causes an improvement in activity towards tyrosine.

To conclude, two variants with improved monophenolase/diphenolase activity ratio were obtained. The investigation of their structure further demonstrated the importance of position 218 and its effect on H60, which also influences copper ion flux into the active site. The results obtained for variant V218F, which has a significantly decreased diphenolase activity, are especially encouraging from an applicative perspective, as it has great potential to be used in a system for production of commercially valuable substituted catechols.

Supplementary data to this article can be found online at http://dx.doi.org/10.1016/j.bbapap.2012.12.021.

Acknowledgements

This work was supported by the Israel Science Foundation founded by the Israel Academy of Sciences and Humanities, grant number 193/11. We gratefully thank the staff of the ESRF (beamline ID23-1) for provision of synchrotron radiation facilities and assistance.

References

[1] H. Claus, H. Decker, Bacterial tyrosinases, Syst. Appl. Microbiol. 29 (2006) 3–14.
[2] S.G. Burton, Oxidizing enzymes as biocatalysts, Trends Biotechnol. 21 (2003) 543–549.
[3] E. Selinheimo, D. NiEidhin, C. Steffensen, J. Nielsen, A. Lomascolo, S. Halaouli, E. Record, D. O'Beirne, J. Buchert, K. Kruus, Comparison of the characteristics of fungal and plant tyrosinases, J. Biotechnol. 130 (2007) 471–480.
[4] M.V. Martinez, J.R. Whitaker, The biochemistry and control of enzymatic browning, Trends Food Sci. Technol. 6 (1995) 195–200.
[5] H. Decker, F. Tuczek, Tyrosinase/catecholoxidase activity of hemocyanins: structural basis and molecular mechanism, Trends Biochem. Sci. 25 (2000) 392–397.
[6] C. Olivares, J.C. Garcia-Borron, F. Solano, Identification of active site residues involved in metal cofactor binding and stereospecific substrate recognition in mammalian tyrosinase. Implications to the catalytic cycle, Biochemistry 41 (2002) 679–686.
[7] C. Olivares, F. Solano, New insights into the active site structure and catalytic mechanism of tyrosinase and its related proteins, Pigment Cell Melanoma Res. 22 (2009) 750–760.
[8] H. Decker, T. Schweikardt, D. Nillius, U. Salzbrunn, E. Jaenicke, F. Tuczek, Similar enzyme activation and catalysis in hemocyanins and tyrosinases, Gene 398 (2007) 183–191.
[9] S. Itoh, S. Fukuzumi, Monooxygenase activity of type 3 copper proteins, Acc. Chem. Res. 40 (2007) 592–600.
[10] K.E. van Holde, K.I. Miller, H. Decker, Hemocyanins and invertebrate evolution, J. Biol. Chem. 276 (2001) 15563–15566.
[11] T. Klabunde, C. Eicken, J.C. Sacchettini, B. Krebs, Crystal structure of plant catechol oxidase containing a dicopper center, Nat. Struct. Biol. 5 (1998) 1084–1090.
[12] S. Halaouli, M. Asther, J.C. Sigoillot, M. Hamdi, A. Lomascolo, Fungal tyrosinases: new prospects in molecular characteristics, bioengineering and biotechnological applications, J. Appl. Microbiol. 100 (2006) 219–232.
[13] Y. Kawamura-Konishi, M. Tsuji, S. Hatana, M. Asanuma, D. Kakuta, T. Kawano, E.B. Mukouyama, H. Goto, H. Suzuki, Purification, characterization, and molecular cloning of tyrosinase from *Pholiota nameko*, Biosci. Biotechnol. Biochem. 71 (2007) 1752–1760.
[14] L.C. Nolan, K.E. O'Connor, Use of *Pseudomonas mendocina*, or recombinant *Escherichia coli* cells expressing toluene-4-monooxygenase, and a cell-free tyrosinase for the synthesis of 4-fluorocatechol from fluorobenzene, Biotechnol. Lett. 29 (2007) 1045–1050.
[15] G. Wang, A. Aazaz, Z. Peng, P. Shen, Cloning and overexpression of a tyrosinase gene *mel* from *Pseudomonas maltophila*, FEMS Microbiol. Lett. 185 (2000) 23–27.
[16] C.A. Ramsden, M.R.L. Stratford, P.A. Riley, The influence of catechol structure on the suicide-inactivation of tyrosinase, Org. Biomol. Chem. 7 (2009) 3388–3390.
[17] D. Hernandez-Romero, A. Sanchez-Amat, F. Solano, A tyrosinase with an abnormally high tyrosine hydroxylase/dopa oxidase ratio, FEBS J. 273 (2006) 257–270.
[18] V. Shuster Ben-Yosef, M. Sendovski, A. Fishman, Directed evolution of tyrosinase for enhanced monophenolase/diphenolase activity ratio, Enzyme Microb. Technol. 47 (2010) 372–376.
[19] V. Shuster, A. Fishman, Isolation, cloning and characterization of a tyrosinase with improved activity in organic solvents from *Bacillus megaterium*, J. Mol. Microbiol. Biotechnol. 17 (2009) 188–200.
[20] M. Sendovski, M. Kanteev, V.S. Ben-Yosef, N. Adir, A. Fishman, First structures of an active bacterial tyrosinase reveal copper plasticity, J. Mol. Biol. 405 (2011) 227–237.
[21] M. Sendovski, M. Kanteev, V. Shuster, N. Adir, A. Fishman, Primary X-ray crystallographic analysis of a bacterial tyrosinase from *Bacillus megaterium*, Acta Crystallogr. Sect. F Struct. Biol. Cryst. Commun. 66 (2010) 1101–1103.
[22] J.N. Rodriguez-Lopez, J. Escribano, F. Garciacanovas, A continuous spectrophotometric method for the determination of monophenolase activity of tyrosinase using 3-methyl-2-benzothiazolinone hydrazone, Anal. Biochem. 216 (1994) 205–212.
[23] A.G.W. Leslie, Joint CCP4 + ESF-EAMCB Newsletter on protein crystallography, 1992. (No. 26).
[24] A.J. McCoy, Solving structures of protein complexes by molecular replacement with Phaser, Acta Crystallogr., Sect. D Biol. Crystallogr. 63 (2007) 32–41.
[25] P.D. Adams, P.V. Afonine, G. Bunkoczi, V.B. Chen, I.W. Davis, N. Echols, J.J. Headd, L.W. Hung, G.J. Kapral, R.W. Grosse-Kunstleve, A.J. McCoy, N.W. Moriarty, R. Oeffner, R.J. Read, D.C. Richardson, J.S. Richardson, T.C. Terwilliger, P.H. Zwart, PHENIX: a comprehensive Python-based system for macromolecular structure solution, Acta Crystallogr., Sect. D Biol. Crystallogr. 66 (2010) 213–221.
[26] P. Emsley, K. Cowtan, *Coot*: model-building tools for molecular graphics, Acta Crystallogr., Sect. D Biol. Crystallogr. 60 (2004) 2126–2132.
[27] Y. Matoba, T. Kumagai, A. Yamamoto, H. Yoshitsu, M. Sugiyama, Crystallographic evidence that the dinuclear copper center of tyrosinase is flexible during catalysis, J. Biol. Chem. 281 (2006) 8981–8990.
[28] W.T. Ismaya, H.t.J. Rozeboom, A. Weijn, J.J. Mes, F. Fusetti, H.J. Wichers, B.W. Dijkstra, Crystal structure of *Agaricus bisporus* mushroom tyrosinase: identity of the tetramer subunits and interaction with tropolone, Biochemistry 50 (2011) 5477–5486.
[29] H. Decker, T. Schweikardt, F. Tuczek, The first crystal structure of tyrosinase: all questions answered? Angew. Chem. Int. Ed Engl. 45 (2006) 4546–4550.
[30] J.L. Muñoz-Muñoz, J. Berna, F. Garcia-Molina, P.A. Garcia-Ruiz, J. Tudela, J.N. Rodriguez-Lopez, F. Garcia-Canovas, Unravelling the suicide inactivation of tyrosinase: a discrimination between mechanisms, J. Mol. Catal. B: Enzym. 75 (2012) 11–19.
[31] C.A. Ramsden, P.A. Riley, Mechanistic studies of tyrosinase suicide inactivation, Arkivoc 1 (2010) 260–274.
[32] J.L. Muñoz-muñoz, F. García-molina, P.A. García-ruiz, M. Molina-alarcón, J. Tudela, F. García-cánovas, J.N. Rodríguez-lópez, Phenolic substrates and suicide inactivation of tyrosinase: kinetics and mechanism, Biochem. J. 416 (2008) 431–440.